Spallation of copper by 80-GeV ^{40}Ar Ions

J. B. Cumming, P. E. Haustein, T. J. Ruth, and G. J. Virtes*
Chemistry Department, Brookhaven National Laboratory, Upton, New York 11973
(Received 1 December 1977)

Cross sections for the production of 35 radioactive nuclides extending from ^{7}Be to ^{67}Ga by the interaction of 80-GeV ^{40}Ar ions with Cu have been measured. These are compared with existing results for other relativistic heavy ions and for 28-GeV protons incident on Cu targets of various thicknesses. Differences in shapes of the yield distributions for products with $37 \leq A \leq 64$ are inferred to arise primarily from increased secondary effects in the semithick targets used for the heavy-ion studies. The larger absolute cross sections (corrected to zero target thickness) for ^{40}Ar ions appear to be due solely to the increased total reaction cross section, σ_R, over that for protons. The production of target fragments with $22 \leq A \leq 64$ is estimated to account for $\approx 70\%$ of σ_R. Calculations using realistic nuclear density distributions suggest that such products are formed in peripheral collisions (impact parameters $\gtrsim 5$ fm) in which there is no strong overlap of the cores of the ^{40}Ar and Cu nuclei. Lighter products are presumed to result from more central collisions, and these are enhanced by factors larger than expected from σ_R (a factor of 2 greater in the case of ^{7}Be). The application of the concepts of limiting fragmentation and factorization as a framework for the interpretation of high-energy heavy-ion induced reactions with complex nuclei is discussed.

[NUCLEAR REACTIONS Cu(^{40}Ar, spallation), $E = 80$ GeV; measured $\sigma(A,Z)$, 35 products ^{7}Be–^{67}Ga; deduced mass yield and charge dispersion curves, target fragmentation cross sections. Natural targets, Ge(Li) counting, radiochemistry.]

I. INTRODUCTION

Studies of the interaction of complex nuclei at energies of hundreds to thousands of MeV per nucleon have been made possible by the acceleration of heavy ions to relativistic energies. Considerable interest in high-energy heavy ion collisions stems from suggestions[1-7] that these projectiles may be capable of inducing new phenomena such as nuclear shock waves, states of abnormal nuclear density, etc. To date, such exotic processes appear to have escaped detection, yet reactions of many diverse types have been observed. These range from the relatively gentle removal of a single nucleon from an energetic projectile by Coulomb excitation[8] to violent interactions leading to the explosion of a target nucleus into multiple small fragments.[9] It is convenient to group the observed products into three classes: projectile fragments, target fragments, and products arising from composite systems containing highly excited matter from both projectile and target.

In the first of these classes, projectile fragments are observed to be collimated strongly near zero degrees in the laboratory system with velocities close to that of the incident ion.[10] Relative yields and spectra of individual fragments are independent of target, while absolute yields are independent of projectile energy in the range 1–2 GeV/nucleon and vary only slowly with target mass[11] (about as $A_T^{1/4}$). These observations suggest the applicability of the ideas of limiting fragmentation and factorization which had been developed initially to account for similar phenomena in peripheral reactions between elementary particles at high energies.[12]

The same general behavior is expected for the second class of products, target fragments, but with the roles of target and projectile reversed. Early studies of Cu irradiated with 3.9-GeV ^{14}N ions[13] showed a relative yield pattern similar to that for high-energy protons, with the exception that yields of light fragments, ^{3}H and ^{7}Be, were enhanced. Similar results have been obtained in radiochemical studies of 25-GeV ^{12}C ions incident on Cu,[14] Ag,[15] Au,[16] and Pb.[16] However, data for U targets[17] have been interpreted as showing a prominent peak for products with $160 \leq A \leq 190$ which is not found in proton irradiations. On the other hand, mica track detector experiments[18] have shown that the fission of Au, Bi, and U by 28-GeV ^{14}N ions is very similar to that induced by protons, with the exception that cross sections are larger by the ratio of total reaction cross sections. With the exception of the anomalous peak for U,[17] these results are again consistent with the factorization hypothesis.

Significant differences between proton and heavy-ion interactions are observed for the third class of products, those species which appear to be associated with partial amalgamation of projectile and target. Poskanzer and co-workers[19-22] have extensively studied the emission of energetic protons and light fragments as probes of the creation

of regions of highly excited nuclear matter. Not only are light fragments emitted more copiously in heavy-ion reactions, but their spectra are harder as well. For example, the yield of ^{7}Li from U at 90° is ≈12 times larger for an incident ^{20}Ne than for a proton, and the temperature inferred for the emitting system is 15 MeV for ^{20}Ne compared with 10 MeV for protons.[22] Such differences, while pronounced, are more of degree rather than kind. Westfall *et al.*[20] have shown that the spectra and numbers of energetic protons produced in heavy-ion reactions can be predicted by the fireball model (at bombarding energies up to 400 MeV/nucleon but not at 2.1 GeV/nucleon). Furthermore, the spectra and numbers of energetic heavier fragments could be accounted for in terms of a coalescence of nucleons having the energy spectrum observed for protons.[21]

The present experiment represents an extension of previous studies of Cu fragmentation by heavy ions[13,14] to a system in which the projectile and target are of comparable mass. Because cross sections have been measured rather than the relative yields reported previously for ^{12}C and ^{14}N ions, absolute enhancement of individual yields over the values for high-energy protons can be calculated as a test of factorization. A total cross section for the target fragmentation process can also be obtained from the mass yield curve deduced in this work.

II. EXPERIMENTAL PROCEDURES AND RESULTS

A target containing Al, Cu, and Mylar foils was irradiated with 80-GeV ^{40}Ar ions in the external beam of the LBL Bevalac. The target foils were 5 cm square and their thicknesses and orders were as indicated in Table I. During the 497-min irradiation a nearly constant flux of approximately 6×10^{7} particles per min passed through the target.

TABLE I. Properties of the target stack. The ^{40}Ar beam passed through the stack from foil 1 to foil 11.

Foil	Material	Thickness (mg/cm^2)
1	Al	4.8
2	Al	42.7
3	Al	4.7
4	Mylar	17.5
5	Mylar	17.7
6	Cu	9.3
7	Cu	233.9
8	Cu	234.4
9	Cu	9.3
10	Mylar	17.6
11	Mylar	17.6
Total		609.5

After irradiation the target was flown to Brookhaven and circles 2.7 cm in diameter centered on the beam spot were punched out.

γ-ray assays were begun 14 hours after the end of bombardment. The detectors and analysis procedures were identical to those used previously.[13,14] Initially, Cu foil 7 was counted on one Ge(Li) detector system and foil 8 on another. After 8 hours, foil 7 was dissolved for radiochemical analyses of ^{64}Cu and ^{56}Ni, while the counting of foil 8 continued. About 24 hours later a series of periodic exchanges of foil 8 between the two detector systems was initiated and continued for ≈3 months. After completion of γ counting, foil 8 was melted for the extraction and analysis of argon isotopes. The shortest-lived nuclide which was observed in this work was ^{56}Mn (2.56-h half-life), the longest, ^{39}Ar (269-yr half-life).

The energy loss of ^{10}Ar ions in traversing the target was ≈0.3 GeV and fragments from the breakup of the projectile should not have been retained by the foil stack. Mylar foils numbered 5 and 10 in Table I were intended to catch recoils from the Cu. While some net activity was observed compared with Mylar 11 which served as a blank, the low levels precluded accurate measurements. The mean ranges of products, as given approximately by the quantity[23] $2w(F+B)$, were found to be the order of a few mg/cm^2 of Cu, indicating that we are observing relatively low energy recoils and that the guard foils (Cu 6 and 9) are thick enough to compensate for recoil losses of products as light as ^{24}Na. That activities were not depleted in Cu 7 compared to Cu 8 is evidence for the absence of more energetic forward peaked recoils which might not have been stopped by Mylar foils 10 to 11. Previous studies[13,14] with protons and ^{14}N and ^{12}C ions suggest that recoil losses of ^{7}Be (which was determined in Cu 8) can also be ignored.

The cross sections obtained in this work are listed in Table II in the column headed 609 mg/cm^2. The half-lives and γ-ray abundances used in calculating disintegration rates were those listed in the compilation by Bowman and MacMurdo[24] with a few exceptions. ^{24}Na production in Al foil 2 served as the beam monitor. On the basis of the 27 ± 4-mb cross section for the ^{27}Al(^{40}Ar,X)^{24}Na reaction reported by Katcoff,[25] the total fluence was determined to be 2.9×10^{10} ^{40}Ar ions. Standard errors assigned to the cross sections are based on our estimates of errors from counting statistics, resolution of γ-ray spectra, etc., or on the agreement of multiple determinations whichever was larger. They do not, in general, include systematic effects such as the uncertainties in the monitor cross section or γ-ray abundances. How-

TABLE II. Cross sections in mb for the production of various isotopes by the interactions of 80-GeV ^{40}Ar ions with Cu in target thicknesses as indicated. Cross sections were calculated for the natural isotopic abundance of copper. Errors do not include the 15% uncertainty in the monitor cross section.

Isotope	Target thickness 609 mg/cm^2	0 mg/cm^2 [a]
^{7}Be	76. ± 2	94. ± 6
^{22}Na	12. ± 5	14. ± 6
^{24}Na	12.3 ± 0.2	15.0 ± 1.0
^{28}Mg	1.50 ± 0.08	1.84 ± 0.15
^{37}Ar	10.7 ± 0.3	13.2 ± 0.9
^{39}Ar	19.5 ± 3.9	23.9 ± 5.0
^{42}K	10.3 ± 0.7	12.6 ± 1.2
^{43}K	3.20 ± 0.10	3.85 ± 0.25
^{43}Sc	9.4 ± 3.8	8.5 ± 3.5
^{44}Sc^{m}	12.6 ± 0.2	15.1 ± 0.8
^{44}Sc^{g}	9.0 ± 1.9	10.7 ± 2.3
^{46}Sc	18.0 ± 0.8	21.0 ± 1.4
^{47}Sc	6.58 ± 0.16	7.56 ± 0.37
^{48}Sc	1.53 ± 0.14	1.73 ± 0.17
^{48}V	23.7 ± 0.4	26.8 ± 1.1
^{48}Cr	0.81 ± 0.03	0.92 ± 0.05
^{51}Cr	49.8 ± 1.5	51.9 ± 1.7
^{52}Mn^{g}	17.2 ± 0.2	17.3 ± 0.2
^{52}Fe	0.35 ± 0.07	0.35 ± 0.07
^{54}Mn	51.0 ± 1.4	47.2 ± 1.8
^{55}Co	3.57 ± 0.20	3.15 ± 0.22
^{56}Mn	10.8 ± 1.7	9.1 ± 1.6
^{56}Co	21.0 ± 1.1	17.6 ± 1.4
^{56}Ni	0.1 ± 0.8	0.1 ± 0.7
^{57}Co	64.6 ± 1.9	51. ± 5
^{57}Ni	2.36 ± 0.28	1.87 ± 0.28
^{58}CO	84.8 ± 1.4	37 ± 7
^{59}Fe	8.3 ± 0.4	5.9 ± 0.9
^{60}Co	46 ± 18	31 ± 13
^{61}Cu	48.7 ± 3.5	32 ± 6
^{62}Zn	3.5 ± 0.4	...
^{64}Cu	84 ± 18	64 ± 15
^{65}Zn	7.2 ± 3.3	...
^{66}Ga	0.8 ± 0.8	...
^{67}Ga	2.8 ± 0.6	...

[a] Details of the procedure used to correct for secondary effects are given in the text.

ever, where several γ rays were assayed for one nuclide, the errors include contributions from uncertainties in both the efficiency and abundance. Reported cross sections are cumulative except for the cases where beta decay feeding of a product is blocked by a long-lived or stable precursor. As observed previously[13,14] such feeding is a small effect.

III. ANALYSIS

A. Comparison of heavy-ion and proton induced spallation: secondary effects

Cross sections measured in the present work (Table II) are substantially larger than those reported for 28-GeV protons incident on thin targets.[14] For example, the ^{61}Cu cross section is 5.4 times the proton value, that of ^{52}Mn^{g} is larger by a factor of 3.7, and that of ^{7}Be is 8.1 times as large. Presumably a major portion of these enhancements is due to the larger total reaction cross section, σ_R, for ^{40}Ar ions (a factor of 3.5).[26-29] Those remaining differences which appear to favor products near the target are due, at least in part, to secondary reactions in the thick targets used for the heavy-ion work. Studies with protons in thick targets[14] reveal shifts of the yield distribution in that direction (as expected from reaction thresholds). On the other hand, it is unlikely that ^{7}Be would be affected by secondary reactions and this represents a real enhancement over that expected on the basis of σ_R alone. Similar patterns of enhancement (although only on relative scales) have been reported for Cu irradiated with 3.9-GeV ^{14}N ions[13] and with 25-GeV ^{12}C ions.[14]

A novel and informative way to study secondary effects quantitatively is to examine correlations between yields of selected nuclides and that of a product which is known to have high sensitivity to secondary reactions. If data for protons incident on targets of various thicknesses and from heavy-ion experiments are included in the same graph, and if a single correlation line is found, then it strongly suggests that the shifts in yields observed for the heavy ions are due to secondary effects.[30] For this analysis we will use cross sections relative to those of ^{52}Mn^{g} to remove, by normalization, large differences due to σ_R and because only relative yields have been measured in some cases. Secondary effects for ^{52}Mn^{g} are nearly identical to those for the commonly used ^{24}Na-from-Al monitor reaction.[14]

It has been proposed[14] that the yield of a trans-copper product such as ^{62}Zn would be an appropriate internal monitor of secondary reactions. As can be seen from the entries for 19- (Ref. 31) and 28-GeV protons in Table III, the relative pri-

TABLE III. Cross sections for forming ^{62}Zn relative to those of ^{52}Mn^{g} by the irradiation of Cu targets of thicknesses indicated with various bombarding particles.

Bombarding particle and energy in GeV	Target thickness (mg/cm^2)	$\frac{\sigma(^{62}\text{Zn})}{\sigma(^{52}\text{Mn}^{g})}$	Graph symbol [a]
^{1}H, 3.9 [b]	183	0.021 ± 0.001	B
^{1}H, 19 [c]	1.8	0.015 ± 0.003	•••
^{1}H, 19 [c]	157	0.037 ± 0.003	•••
^{1}H, 28 [d]	154	0.041 ± 0.004	A
^{1}H, 28 [d]	1158	0.120 ± 0.007	E
^{1}H, 28 [e]	2269	0.141 ± 0.004	G
^{14}N, 3.9 [b]	1056	0.118 ± 0.006	D
^{12}C, 25 [d]	1158	0.214 ± 0.012	F
^{40}Ar, 80 [f]	609	0.204 ± 0.026	C

[a] Used for identification in Fig. 1.
[b] Reference 13.
[c] Reference 31.
[d] Reference 14.
[e] Measurements of relative yields of ^{62}Zn, ^{61}Cu, ^{52}Mn^{g}, ^{44}Sc^{m}, ^{24}Na, and ^{7}Be in targets thicker than those reported in Ref. 14 were made in conjunction with the present work.
[f] Present work.

mary yield of ^{62}Zn is low, 0.015, and nearly 90% of the ^{62}Zn observed in thick targets results from secondary reactions. Most of the ^{62}Zn produced in thick Cu targets irradiated with heavy ions is probably due to secondary reactions as well. Evidence for this is the observation that the transfer of charge or mass from a target to a relativistic heavy ion is an improbable process in projectile fragmentation.[11] Production of ^{62}Zn represents a corresponding reaction in target fragmentation.

Correlations between four representative yields and ^{62}Zn are shown in Fig. 1. Nuclides chosen are ^{61}Cu, typical of near-target products with high primary yields but also sensitive to secondaries; ^{44}Sc^{m}, a deep spallation product with low or no sensitivity to secondaries; and ^{24}Na and ^{7}Be, low mass products representative of interactions involving deposition of large amounts of energy in the target nucleus. In each case the rectangles (filled for protons and open for heavy ions) indicate regions consistent with the measured values and their errors. The straight lines are least-squares fits to the points for 28-GeV protons labeled A, E, and G. These lines indicate the general trends expected for secondary effects. The strong positive slope for ^{61}Cu indicates that it is more influenced by secondary reactions than is ^{52}Mn^{g}, the normalizing reaction product. Negative slopes for ^{44}Sc^{m}, ^{24}Na, and ^{7}Be imply that these species are less sensitive. This is consistent with the previous conclusion[14] that the contribution of secondary reactions decreases as the distance between target and production increases, and becomes insignificant for products with $A \lesssim 40$.

If all points for heavy ions were to fall on or near these proton lines it would suggest similar primary to secondary yield ratios for the heavy-ion reactions. This is indeed the case for ^{61}Cu and ^{44}Sc^{m} where the heavy-ion points are consistent with the proton correlation lines, or with shifts of these lines within experimental uncertainties. It is also true for the other products with $37 \leq A \leq 64$ not shown in Fig. 1. However, there is a significant difference between heavy ions and protons for ^{7}Be. Relative yields for the heavy projectiles are up to a factor of 2 greater than those for protons, with the difference apparently increasing both with energy per nucleon (compare 25-GeV ^{12}C with 3.9 GeV ^{14}N) and with projectile mass (compare 80-GeV ^{40}Ar with 25-GeV ^{12}C). A similar enhancement has been reported for ^{3}H formed by the irradiation of Cu with 3.9-GeV ^{14}N ions.[13] This characteristic fingerprint of energetic heavy-ion interactions has largely disappeared at ^{24}Na.

Points for 3.9-GeV protons (labeled B) and 3.9-GeV ^{14}N ions (labeled D) have been included in Fig. 1 to explore the energy dependence of spallation reactions. For protons it is known[32] that cross sections of products near the target are approximately energy independent in the 3–30-GeV region, but that lighter product yields such as ^{24}Na and ^{7}Be are still rising. Positions of the

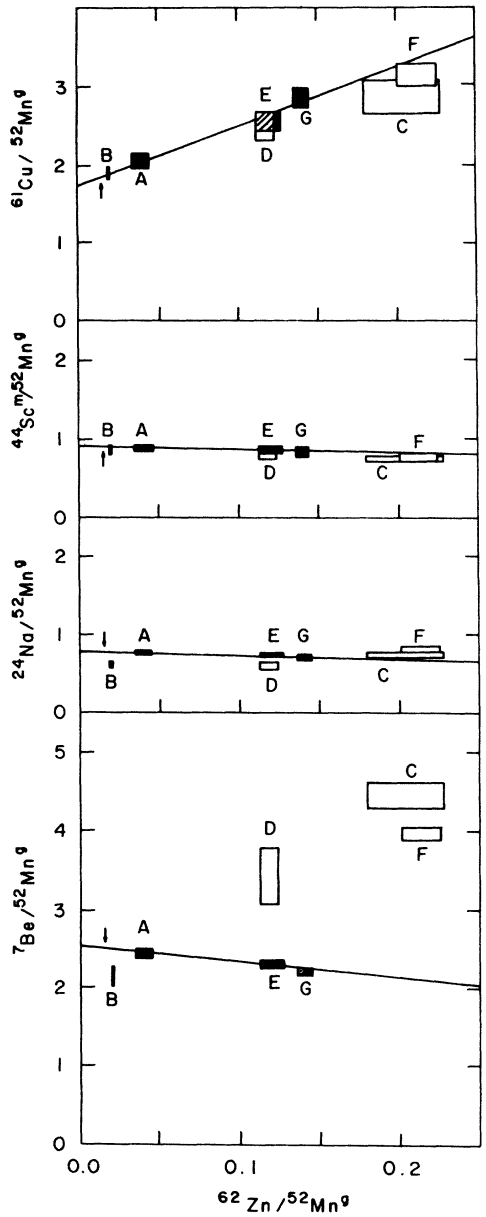

FIG. 1. Correlations between yields of four representative products, ^{61}Cu, $^{44}Sc^m$, ^{24}Na, and ^{7}Be, and ^{62}Zn as an indicator of secondary effects in the spallation of Cu by various bombarding particles. Rectangles (filled for incident protons, open for heavy ions) show areas consistent with the experimental values. The lines are least squares fits to the points for 28-GeV protons labeled A, E, and G. For further details see Table III and text.

B-labeled points with respect to the 28-GeV correlation lines in Fig. 1 confirm this. There is some evidence for the same effect with the heavy ions. Note that the point for ^{24}Na for 3.9-GeV ^{14}N ions falls below the line and the enhancement of ^{7}Be, as noted above, is somewhat less than for 25-GeV ^{12}C ions.

The nearly linear correlation lines in Fig. 1 for products such as ^{61}Cu and $^{44}Sc^m$ suggest that secondary corrections are proportional to the relative ^{62}Zn yield in excess of the thin target value (0.015). We have corrected the cross section measured for ^{40}Ar incident on Cu to thin target values by combining this conclusion with secondary corrections reported previously for protons.[14] For example, the ^{61}Cu cross section measured for protons in an 1158-mg/cm^2 target is 28.7% higher than the thin target value due to contributions from secondary reactions (see Fig. 1 of Ref. 14). From the data in Table III, the secondary reactions in a 609-mg/cm^2 Cu target irradiated with 80-GeV ^{40}Ar ions are (0.204-0.015)/(0.120-0.015) or 1.8 $\pm$ 0.28 times those for protons in the 1158-mg/cm^2 target. The correction to the ^{40}Ar data is then 51.7% and we divide the observed cross section (48.7 $\pm$ 3.5) mb by 1.517 to get (32.1 $\pm$ 6.0) mb for the thin target value. Although the error in the factor 1.8 is only 16% due to the ^{62}Zn measurements, we have increased the error to one-third of the correction to include possible systematic effects in this procedure. Corrected cross sections for 80-GeV ^{40}Ar ions incident on a zero thickness target of Cu are given in column 3 of Table II. We have not applied this approach to the zinc and gallium cross sections as the corrections in these cases are very large. Some justification for the assumption implicit in this procedure that the distribution of secondary reaction products is the same for protons and heavy ions comes from studies of activities induced in Cu outside the central beam spots by 25-GeV ^{12}C ions and 28-GeV protons.[14] Very similar mass distributions of products were observed, but the number per primary interaction was larger for the heavy ions.

B. Tests of factorization

The ideas of factorization and limiting fragmentation were developed initially for the interpretation of reactions between elementary particles. It was suggested by Feynman[33] and by Benecke *et al.*[34] that, if one focused on those products which could be identified as fragments of the target or projectile on the basis of low momentum transfer in either the target or projectile rest frames, simple behavior might be observed at sufficiently high energies. In particular, cross sections were expected to become nearly independent of energy and, more significantly, single particle inclusive spectra of target (or projectile) fragments were predicted to depend on the nature of the projectile (or target) only via a total cross section term.

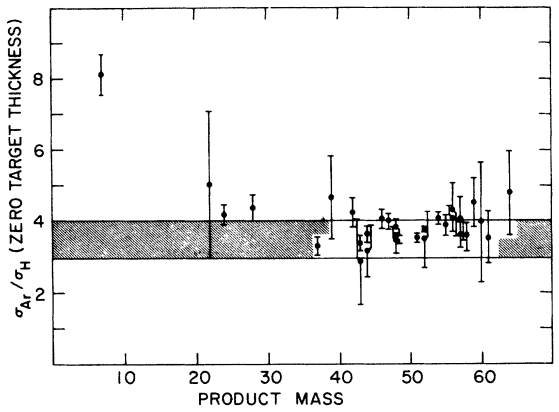

FIG. 2. Cross section ratios vs product mass for the reactions of 80-GeV ^{40}Ar and 28-GeV ^{1}H with Cu. The cross hatched band shows the region consistent with the ratio of total reaction cross sections and its associated error. Data points are calculated from the present work for ^{40}Ar and from Ref. 14 for ^{1}H.

Previous studies of target fragmentation by high-energy heavy ions could not give information on the dependence of yields on the mass or size of the projectile because only relative yields were measured. They did show generally similar yield patterns for heavy-ion and proton irradiations, for example, as could be concluded from Fig. 1. The present work allows more detailed tests. Plotted in Fig. 2 are thin target cross section ratios comparing the production of a given nuclide by 80-GeV ^{40}Ar ions to that by 28-GeV protons. The ratio of total reaction cross sections,[26] σ_R, for these two projectiles is 3.5, and the cross-hatched band in the figure shows the region consistent with that value and the error in the cross section of the ^{27}Al(^{40}Ar,X) ^{24}Na monitor reaction. Of the 26 points shown for products with $37 \leq A \leq 64$, 16 fall in the shaded band and the remaining 10 are within one standard deviation of it. Even the points for ^{22}Na, ^{24}Na, and ^{28}Mg do not deviate much from scaling as σ_R. It is only for the lightest observed product, ^{7}Be, that a deviation by a factor of 2 is observed. This, of course, is a different reflection of the patterns seen in Fig. 1.

The present experiment then gives additional evidence for the validity of factorization as applied to the target fragmentation process. As far as yields of products from copper with $37 \leq A \leq 64$ are concerned, and 80-GeV ^{40}Ar ion looks like an incident proton but with a larger total cross section. What was initially surprising was that the individual nuclide cross sections were found to scale as σ_R. The weaker σ_R dependence observed for the projectile fragmentation process ($\approx \sigma_R^{1/2}$), would have predicted a ratio of 1.9 for the individual cross sections, much lower than that observed.

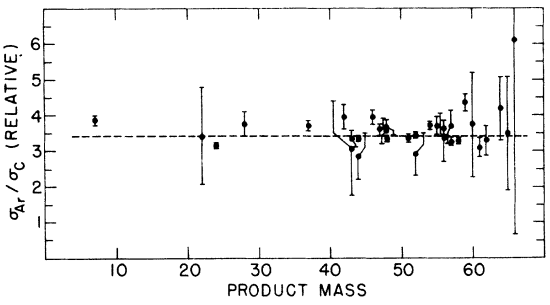

FIG. 3. Relative production rates vs product mass for the reactions of 80-GeV ^{40}Ar (present work) and 25-GeV ^{112}C (Ref. 14) with Cu. The ordinate scale is arbitrary because only relative yields were reported for incident ^{12}C ions. The horizontal, dashed line is the mean of points with $37 \leq A \leq 64$.

We will return to this difference below.

A further test of factorization is a comparison of the present results with those for 25-GeV ^{12}C ions.[14] The data in Table III indicate that secondary effects in the 609-mg/cm^2 target exposed to 80-GeV ^{40}Ar ions in the present work and those in the 1158-mg/cm^2 target used for the ^{12}C study are the same within errors; hence a direct comparison of the experimental data is meaningful. Cross section ratios, σ_{Ar}/σ_C, are plotted in Fig. 3 as a function of product mass. The ordinate scale is arbitrary because only relative yields were measured for the ^{12}C ions. Although the points scatter somewhat, there is no evidence of a trend with mass. Twenty-one of the 29 points fall within 10% of the mean value, 3.42, shown by the dashed line in the figure.[35] It can be inferred from Figs. 2 and 3 that the characteristic fingerprint of heavy-ion interactions with Cu, the enhanced production of light fragments such as ^{7}Be, is well developed for incident ^{12}C ions, and that further increases in projectile size to ^{40}Ar result in at most small changes in relative yield distributions.

It follows from the constancy of the ratios in Figs. 2 and 3 that the same charge dispersion curve will fit the yields for ^{1}H, ^{12}C, and ^{40}Ar ions in the target fragmentation region ($A \gtrsim 37$). This is illustrated in Fig. 4 where points for ^{40}Ar incident on the 609-mg/cm^2 target are superimposed on the CD curve derived previously for 28-GeV protons.[14] The computer fitting procedures used for this analysis have been described elsewhere.[13,14] These procedures were also used to obtain the mass yield curves shown in Fig. 5. These are for thin targets; in the case of ^{12}C ions, published thick target results[14] were corrected by the procedures developed in Sec III A. As expected the curves for the three projectiles have very nearly the same shape except for a vertical displacement which in the case of ^{1}H and ^{40}Ar scales as σ_R.

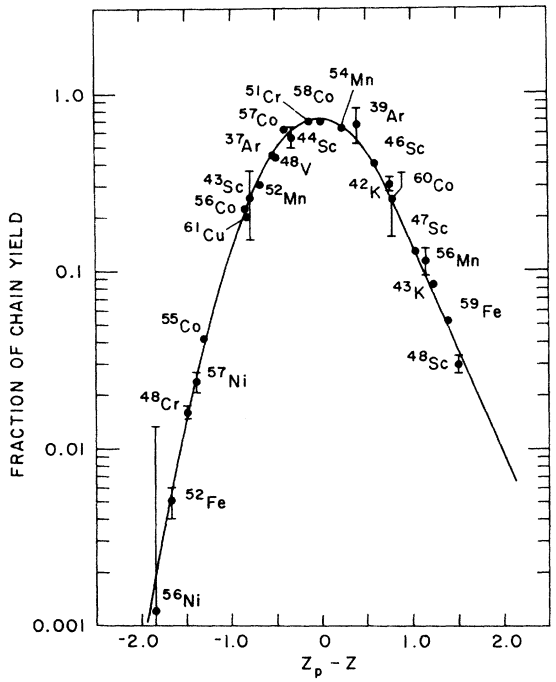

FIG. 4. Comparison of charge dispersion curves for the spallation of Cu by 80-GeV ^{40}Ar and 28-GeV ^{1}H. Points were obtained by the procedure described in Ref. 14 for ^{40}Ar incident on a 609-mg/cm^2 target. The curve is that reported (Ref. 14) for protons on a zero thickness target.

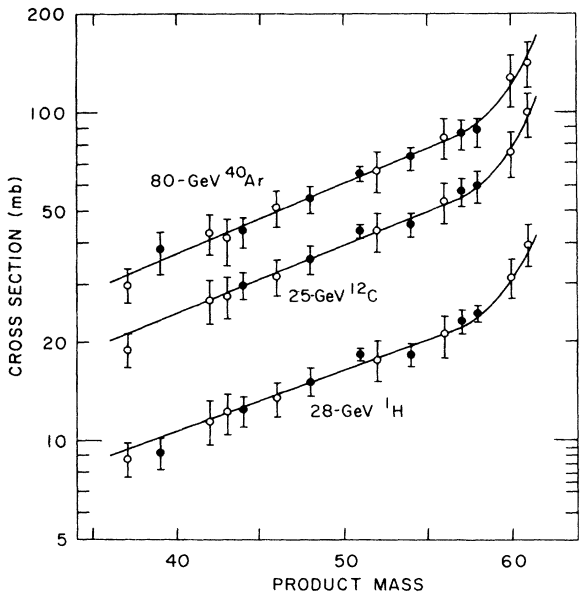

FIG. 5. Mass yield curves for the spallation of Cu by 80-GeV ^{40}Ar (this work), 25-GeV ^{12}C (Ref. 14), and 28-GeV ^{1}H (Ref. 14). The vertical scale for ^{12}C is arbitrary. Points were obtained using the procedure of Ref. 14 by adding computer generated values for non-observed products to the measured cross sections. These are filled when >50% of the total was observed, open when >20% observed. Errors include 20% uncertainties assumed in the calculated values.

The slope of a mass yield curve in the exponential region between $A \approx 37$ and ≈ 57 is an approximate measure of the excitation energy transferred from the bombarding particle: a smaller slope corresponding to greater average mass loss, hence, higher average deposition energy and vice versa. Plotted in Fig. 6 are slopes derived by analyses such as that above for the spallation of Cu by 350-MeV,[36] 590-MeV,[37] 2.2-GeV,[38] 3.9-GeV,[13] 5.7-GeV,[39] 24-GeV,[40] and 28-GeV protons[14] (filled circles) and for 410- and 720-MeV ^{4}He,[41] 3.9-GeV ^{14}N,[13] 25-GeV ^{12}C,[14] and 80-GeV ^{40}Ar (open circles). The onset of energy independence (limiting fragmenation) in the GeV region is apparent, as is the general similarity of heavy-ion and proton values.

The total cross section for the target fragmentation process can be estimated from the mass yield curve. Some 1620 mb of cross section (based on the smooth curve in Fig. 5) is associated with products in the $37 \leq A \leq 61$ region. An additional ≈ 540 mb is estimated to lead to species closer to the target or in the region extending down to $A = 22$. Cross sections in the latter region were obtained by extrapolating the exponential mass yield curve below $A = 37$.[42] The sum, ≈ 2160 mb, represents $\approx 70\%$ of σ_R; hence processes leading to at least one massive residue are very probable in the interaction of relativistic heavy ions with Cu. Interestingly enough, a similar analysis gives a nearly identical fraction of σ_R for incident protons.

IV. DISCUSSION

A variety of detailed theoretical approaches are currently being explored to describe high-energy

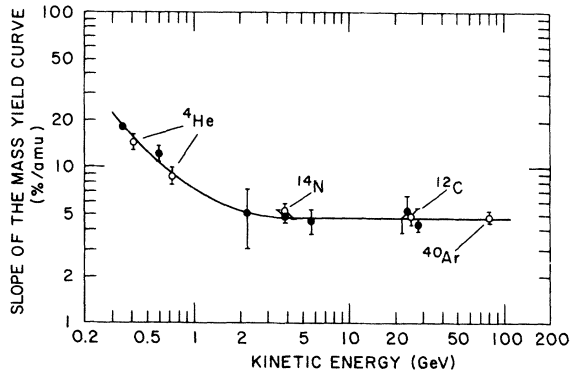

FIG. 6. Slope of the Cu spallation mass yield curve as a function of the kinetic energy of the incident projectile. Filled circles are for protons, open for heavy ions as indicated. Procedures and sources of the data are indicated in the text.

heavy-ion collisions. Results from some of these have been discussed by Amsden *et al.*[43] For discussion of the present results it is convenient to fall back to simpler, physically more pictorial models. In the abrasion-ablation model of Bowman, Swiatecki, and Tsang,[44] the initial interaction of the target and projectile results is a shearing off (abrasion) of the overlapping regions of the nuclei leaving distorted, excited prefragments which subsequently deexcite (ablate) to the observed products. This model and other simple ones for heavy-ion interactions suggest a monotonic relationship (on the average) between impact parameter b and reaction product, with the simplest (smallest mass loss) being associated with the largest b, and vice versa. Based on the procedure of Barshay *et al.*[27,28] in which

$$d\sigma_R = 2\pi b\{1 - \exp[-T(b)\sigma_{NN}^T]\}\,db\,,$$

we have calculated the contributions of different ranges of impact parameters to σ_R. In this equation, $T(b)$ is the thickness function [as defined by Eq. (2.3) of Ref. 28] which includes all the geometrical properties of the colliding nuclei,[45] and σ_{NN}^T is the spin and isospin averaged nucleon-nucelon cross section at 2 GeV/nucleon. This calculation predicts that impact parameters of ≈ 8.2 fm make the largest contributions to σ_R. For closer approaches, the nuclei are black to each other and the b term in the above equation is dominant. For larger b, transparencies become significant, rapidly reducing the contributions, yet some reactions at impact parameters in the 10–12-fm range are expected. We note that the most effective impact parameters are larger than the sum of the half-density radii of ^{40}Ar and ^{63,65}Cu, 3.39 and 4.23 fm, respectively, so that peripheral collisions are expected to play important roles. Impact parameters $\gtrsim 8.3$ fm contribute a cross section equal to the estimated yields of products with $A \geq 58$, the upturning region of the mass yield curve in Fig. 5. Furthermore, the ≈ 2160 mb deduced for target fragmentation residues having $A \geq 22$ are accounted for by collisions with $b \geq 5.25$ fm. Shown in Fig. 7 are realistic nuclear density distributions[46] for Cu and ^{40}Ar at this impact parameter. There is little overlap of the central cores of the projectile and target even at this separation and in this sense target fragmentation is peripheral. Major parts of the Ar and Cu remain relatively undisturbed to ultimately yield the fragmentation products. Presumably events with smaller b and greater overlap will result in increasingly violent interactions. This is consistent with the classical equation-of-motion calculations of Bodmer and Panos[47] for the $A = 50$ on $A = 50$ system. They characterize collisions with

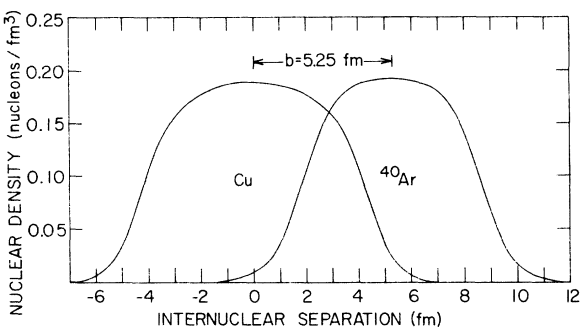

FIG. 7. Nuclear density distributions for Cu and ^{40}Ar showing the extent of overlap when the separation of centers is 5.25 fm.

$b \lesssim 4.2$ fm as "explosive" and note the absence of any large prefragments for $b \leq 2.1$ fm. It is in the collisions at small impact parameters that the greatest difference between heavy ions and protons might be expected, and the production of light fragments such as ^{7}Be may be one of the signatures of such near-central collisions.

That the total cross section for target fragmentation is proportional to σ_R for ^{1}H and ^{40}Ar incident on Cu is not surprising. For a target as light as Cu the skin is comparable in linear dimensions to the core and we measure a major fraction of σ_R for all projectiles up to ^{40}Ar. We would expect that, if Cu were irradiated with heavier projectiles such as Kr or Xe, scaling of the target fragmentation cross section would drop below σ_R and approach the $\sigma_R^{1/2}$ dependence observed for the fragmentation of ^{12}C and ^{16}O projectiles.[10,11] Implicit in the above is our assignment of most of the observed yields to the target fragmentation process. The limited recoil data obtained in the present work suggest there is little momentum transfer from projectile to target for products even as light as ^{24}Na, but clearly more detailed studies are desirable.

It is more difficult to gain a physical picture[48] of the reasons for factorization of the individual fragmentation cross sections, i.e., the single particle inclusive reactions. For example, the fireball version[20] of abrasion-ablation predicts very different mass distributions for the prefragments of Cu irradiated with ^{40}Ar and protons. To obtain the observed factorizability, some mechanism would have to be found for giving the prefragments much higher excitation energies for incident protons than for ^{40}Ar. Feshbach and Huang[49] have noted the equivalence between factorization and the statistical (compound nucleus) theory of nuclear reactions. Such a model, which emphasizes the roles of binding energies and level densities, can account for many of the pro-

perties of projectile fragments.[50-52] The present observation that CD and Z_p curves are independent of bombarding particle suggests the same factors play important roles, at least in the final de-excitation stages of target fragmentation reactions. There is again a problem, however, of why very different projectiles give the same distributions of excited systems.

Some of the difficulties with models at their present state of development have been noted recently by Rasmussen, Donangelo, and Oliveira,[53] who calculated target fragmentation cross sections for ^{12}C incident on ^{40}Ca. Even with the refined fire-steak version[54] of abrasion-ablation, and including contributions of excess surface area[55] and final state interactions[56] to prefragment excitation energies, and contributions from a single fragmentation process (abrasion-ablation is a double fragmentation process in the sense that, for a wide range of impact parameters, projectile fragmentation is correlated with target fragmentation), fits to the experimental data were not fully satisfactory.

The present experimental data, which show that target fragmentation accounts for a major part of the reaction cross section, place significant constraints on possible models. In pointing out the similarities between heavy-ion and proton interactions we stress the need for future theoretical developments in which the transition from elementary particle probes such as pions and protons, to deuterons and α particles, and to more complex nuclei is made in a consistent and continuous way.

The authors particularly wish to acknowledge the efforts of W. Everette, F. Lothrop, and the Bevalac staff in obtaining the ^{40}Ar irradiation and for arranging the prompt shipment of the target to BNL. We are indebted to R. W. Stoenner for assay of the Ar isotopes, E. Norton for chemical yield determinations, and E. Rowland and M. Kinney for assistance in data acquisition and processing. This research was carried out, in part, at Brookhaven National Laboratory under contract with the U. S. Department of Energy and was supported by its Division of Basic Energy Sciences.

---

*Present address: Ward Melville High School, Setauket, New York 11733.

[1]C. Y. Wong and T. A. Welton, Phys. Lett. 49B, 243 (1974).
[2]H. G. Baumgardt, J. U. Schott, Y. Sakamoto, E. Schopper, H. Stocker, J. Hofman, W. Schied, and W. Greiner, Z. Phys. A273, 359 (1975).
[3]M. J. Sobel, P. J. Siemens, J. P. Bondorf, and H. A. Bethe, Nucl. Phys. A251, 502 (1975).
[4]G. Chapline, M. Johnson, E. Teller, and M. Weiss, Phys. Rev. D 8, 4302 (1972).
[5]T. D. Lee and G. C. Wick, Phys. Rev. D 9, 2291 (1974).
[6]T. D. Lee, Rev. Mod. Phys. 47, 267 (1975).
[7]B. Müller, R. K. Smith, and W. Greiner, Lawrence Berkeley Report No. LBL-3675, 1973 (unpublished) p. 109.
[8]H. H. Heckman and P. J. Lindstrom, Phys. Rev. Lett. 37, 56 (1976).
[9]H. H. Heckman, H. J. Crawford, D. E. Greiner, P. J. Lindstrom, and L. W. Wilson, Lawrence Berkeley Report No. LBL-6561, 1977 (unpublished).
[10]D. E. Greiner, P. J. Lindstrom, H. H. Heckman, B. Cork, and F. S. Bieser, Phys. Rev. Lett. 35, 152 (1975).
[11]P. J. Linstrom, D. E. Greiner, H. H. Heckman, B. Cork, and F. S. Bieser, Lawrence Berkeley Laboratory Report No. LBL-3650, 1975 (unpublished).
[12]See the review by H. Bøggild and T. Ferbel, Annu. Rev. Nucl. Sci. 24, 451 (1974).
[13]J. B. Cumming, P. E. Haustein, R. W. Stoenner, L. Mausner, and R. A. Naumann, Phys. Rev. C 10, 739 (1974).
[14]J. B. Cumming, R. W. Stoenner, and P. E. Haustein, Phys. Rev. C 14, 1554 (1976).
[15]C. R. Rudy and N. T. Porile, Phys. Lett. 59B, 240 (1975).
[16]W. Loveland, R. J. Otto, D. J. Morrissey, and G. T. Seaborg, Phys. Lett. 69B, 284 (1977).
[17]W. Loveland, R. J. Otto, D. J. Morrissey, and G. T. Seaborg, Phys. Rev. Lett. 39, 320 (1977).
[18]S. Katcoff and J. Hudis, Phys. Rev. C 14, 628 (1976).
[19]A. M. Poskanzer, R. G. Sectro, A. M. Zebelman, H. H. Gutbrod. A. Sandoval, and R. Stock, Phys. Rev. Lett. 35, 1701 (1975).
[20]G. D. Westfall, J. Gosset, P. J. Johansen, A. M. Poskanzer, W. G. Meyer, H. H. Gutbrod, A. Sandoval, and R. Stock, Phys. Rev. Lett. 37, 1202 (1976).
[21]H. H. Gutbrod, A. Sandoval, P. J. Johansen, A. M. Poskanzer, J. Gosset, W. G. Meyer, G. D. Westfall, and R. Stock, Phys. Rev. Lett. 37, 667 (1976).
[22]J. Gosset, H. H. Gutbrod, W. G. Meyer, A. M. Poskanzer, A. Sandoval, R. Stock, and G. D. Westfall, Phys. Rev. C 16, 629 (1977).
[23]J. M. Alexander, in *Nuclear Chemistry*, edited by L. Yaffe (Academic, New York, 1968), Vol. I, p. 273.
[24]W. W. Bowman and K. W. MacMurdo, Atom. Nucl. Data 13, 89 (1974).
[25]S. Katcoff, private communication.
[26]The total reaction cross section for $^{40}Ar+Cu$ was taken to be 2970 mb based on the calculations of Refs. 27–29. The value for $^{1}H+Cu$, 850 mb, is the experimental value reported by G. Bellettini, G. Cocconi, A. N. Diddens, E. Lillethun, G. Matthiae, J. P. Scanlon, and A. M. Wetherell, Nucl. Phys. 79, 609 (1966).
[27]S. Barshay, C. B. Dover, and J. P. Vary, Phys. Lett. 51B, 5 (1974).

[28]S. Barshay, C. B. Dover, and J. P. Vary, Phys. Rev. C 11, 360 (1975).
[29]P. J. Karol, Phys. Rev. C 11, 1203 (1975).
[30]This approach was suggested to us by a technique developed to infer a common origin (or different origins) for members of a group of outwardly similar artifacts, see G. Harbottle, in *Radiochemistry*, edited by G. W. A. Newton (The Chemical Society, London, 1976), Vol. III, p. 33–72.
[31]G. Rudstam, Nucl. Phys. 56, 593 (1964).
[32]J. Hudis, I. Dostrovsky, G. Friedlander, G. R. Grover, N. T. Porile, L. P. Remsberg, R. W. Stoenner, and S. Tanaka, Phys. Rev. 129, 434 (1963).
[33]R. P. Feynman, Phys. Rev. Lett. 23, 1415 (1969).
[34]J. Benecke, T. T. Chou, C. N. Yang, and E. Yen, Phys. Rev. 188, 2159 (1969).
[35]The present data and the factorization hypothesis can be used to estimate a cross section for the ^{27}Al(^{12}C, X)^{24}Na reaction. This had arbitrarily been taken as equal to the proton value, 8.0 mb, in the previous work. Calculations indicate σ_R for ^{40}Ar + Cu will be 1.51 times that for ^{12}C + Cu. The observed relative factorization ratio is 3.42, hence the unknown monitor cross section is $(3.42/1.51)\times 8.0 = 18 \pm 3$ mb. The error here reflects the error in the ^{27}Al(^{40}Ar, X)^{24}Na cross section which enters via the factor 3.42.
[36]C. J. Orth, private communication.
[37]J. E. Cline and E. B. Nieschmidt, Nucl. Phys. A169, 437 (1971); C. J. Orth, H. A. O'Brien, Jr., M. E. Schillaci, B. J. Dropesky, J. E. Cline, E. B. Nieschmidt, and R. L. Brodzinski, J. Inorg. Nucl. Chem. 38, 13 (1976); C. J. Orth (unpublished).
[38]G. Friedlander, J. M. Miller, R. Wolfgang, J. Hudis, and E. Baker, Phys. Rev. 94, 727 (1954).
[39]D. W. Barr, Lawrence Berkeley Report No. UCRL 3793, 1957 (unpublished).
[40]G. Rudstam, Phys. Rev. 126, 1852 (1962).
[41]P. J. Karol, Phys. Rev. C 10, 150 (1974).
[42]The general systematics of spallation yields indicate that mass yield curves turn up at low masses. Extrapolation of the lines in Fig. 5 appears to underestimate cross sections at $A \approx 23$ by $\approx 20\%$ for ^{1}H and by $\approx 70\%$ for ^{40}Ar. However, some of these light products may well have heavier partners or represent residues of near central collisions and as such should not be counted as target fragmentation residues.
[43]A. A. Amsden, J. N. Ginocchio, F. H. Harlow, J. R. Nix, M. Danos, E. C. Halbert, and R. K. Smith, Jr., Phys. Rev. Lett. 38, 1055 (1977). This gives references to a variety of other calculations.
[44]J. D. Bowman, W. J. Swiatecki, and C. F. Tsang, Lawrence Berkeley Report No. LBL-2908, 1973 (unpublished).
[45]We are indebted to C. Dover for numerical values of $T(b)$ for the ^{40}Ar + Cu system.
[46]These are based on results of electron scattering experiments: for ^{40}Ar, from J. L. Groh, R. P. Singhal, and H. S. Caplan, Can. J. Phys. 49, 2073 (1971); for ^{63,65}Cu, we have used results for ^{64}Ni from J. R. Ficenec, W. P. Trower, J. Heisenberg, and I. Sick, Phys. Lett. 32B, 460 (1970).
[47]A. R. Bodmer and C. N. Panos, Phys. Rev. C 15, 1342 (1977).
[48]A. H. Mueller, Phys. Rev. D 2, 2963 (1970, has discussed single particle inclusive reactions in terms of three particle → three particle amplitudes. In this analysis, factorization is a consequence of a reaction proceeding via a single factorizable exchange mechanism.
[49]H. Feshbach and H. Huang, Phys. Lett. 47B, 300 (1973).
[50]R. K. Bhaduri, Phys. Lett. 50B, 211 (1974).
[51]A. S. Goldhaber, Phys. Lett. 53B, 306 (1974).
[52]N. Masuda and F. Uchiyama, Phys. Rev. C 15, 972 (1977).
[53]J. Rasmussen, R. Donangelo, and L. Oliveira, Lawrence Berkeley Report No. LBL-6580, 1977 (unpublished).
[54]W. D. Meyers, as quoted in Ref. 53.
[55]W. J. Swiatecki (unpublished).
[56]J. Hüfner, K. Schäfer, and B. Schürmann, Phys. Rev. C 12, 1888 (1975).